Institut de Physique, Université de Neuchâtel

JONCTIONS SUPRACONDUCTRICES A EFFET TUNNEL COMME DETECTEURS DE PARTICULES

Superconducting tunneling junctions as particle detectors

Thèse présentée à la faculté
des sciences de l'Université de Neuchâtel
par Yves de Coulon
pour l'obtention du grade de dr ès sciences, septembre 1989.

en présence du jury composé de MM :
Prof. J.-L. Vuilleumier (directeur de thèse) , Neuchâtel
Prof. P. Martinoli, Neuchâtel
Prof. K.P. Pretzl, Berne
Dr. D. Twerenbold, Neuchâtel

IMPRIMATUR POUR LA THÈSE

Jonctions supraconductrices à effet tunnel comme détecteurs de particules

de M.onsieur Yves de Coulon

UNIVERSITÉ DE NEUCHÂTEL

FACULTÉ DES SCIENCES

La Faculté des sciences de l'Université de Neuchâtel sur le rapport des membres du jury,

Messieurs J.-L. Vuilleumier, P. Martinoli, D. Twerenbold et K. Pretzl (Berne)

autorise l'impression de la présente thèse.

Neuchâtel, le 6 novembre 1989

Le doyen :

Cl. Mermod

List of publications

- Y.de Coulon, D. Twerenbold, J.-L. Vuilleumier and G.A. Racine, Proc. of the II European Workshop on Low Temperature Devices for the Detection of Low Energy Neutrinos and Dark Matter, ed. L. Gonzalez-Mestres and D. Perret-Gallix, Editions Frontières, Gif-sur-Yvette, 1989.

- Y. de Coulon, D. Twerenbold and J.-L. Vuilleumier, Correlation Measurements of Ionizing Radiation induced Phonons in Silicon using Superconducting Tunneling Junctions, submitted to Nuclear Instruments and Methods A.

Ces articles constituent un résumé du travail de thèse pour l'obtention du grade de Docteur ès Sciences de l'Université de Neuchâtel. Le texte complet de ce travail peut être obtenu chez: Prof. J.-L. Vuilleumier, Université de Neuchâtel, Institut de Physique, Rue A.-L. Breguet 1, CH-2000 NEUCHATEL.

Correlation Measurements of Ionizing Radiation induced Phonons in Silicon using Superconducting Tunneling Junctions

Y.de Coulon, D.Twerenbold and J.-L.Vuilleumier

Institut de Physique de l'Université

CH-2000 Neuchâtel, Switzerland

Abstract

Nonthermal phonons produced by X ray and alpha particle absorption in silicon were detected with superconducting Sn/Sn-ox/Sn tunneling junctions. The correlation of signals induced by phonons from the substrate in two closely spaced junctions shows structures indicative of an anisotropic propagation of the nonthermal phonons. Taking into account the geometrical collection efficiency of the small area junctions, more than 60 % of the energy deposited in the crystal is converted into excess quasiparticles.

submitted to Nuclear Instruments and Methods A Neuchâtel, 26-Feb-90

1. Introduction

A new sensitivity range in particle detection has become accessible with the advance of cryogenic detectors. There, the various low energy excitations of solids or liquids at sub Kelvin temperatures offer the possibility for a new class of detectors with high sensitivity and energy resolution. Of importance is especially the sensitivity to nonionizing or poorly ionizing events, e.g. recoiling nuclei, owing to the direct transfer of the particle energy to the phonons, one of the basic entities of solid state cryogenic detectors. In particular, two detector types have demonstrated their feasibility in the last years: the bolometer[1,2,3] and the superconducting tunneling junction detector[4,5,6]. In the bolometer, the energy deposited by the particle is measured by the induced temperature rise in a crystal. Owing to the small specific heat, this temperature rise is large and can be measured with high precision against the low background of phonon fluctuations at those low temperatures. An energy resolution of 17 eV at 6 keV has been achieved[1] at the base temperature of 80 mK. In contrast to the thermal nature of the bolometer, the superconducting tunneling junction detector is based on the nonthermal properties of the basic electronic excitations in a superconductor, the quasiparticles. The basic mechanism is the breaking of Cooper pairs by the deposited energy and the subsequental production of excess quasiparticles. The binding energy of a Cooper pair being 2Δ (Δ is the superconducting gap of the order of meV) leads to a large number Q of excess quasiparticles of the order of E/Δ (E is the energy deposited by the particle). Owing to the Poisson statistical nature of Q, the relative precision in measuring the deposited energy is of the order of $1/\sqrt{Q}$. Theoretically, a resolution of better than 10 eV at 6 keV should be achievable for this detector. The best result[7], obtained for Sn/Sn-Ox/Sn junctions at 400 mK, is 55 eV at 6 keV.

The fact that superconducting tunneling junctions are also sensitive to nonthermal phonons produced by the energy deposited in the crystalline substrate[8,9] suggests a third type of cryogenic detector: a crystal covered with superconducting tunneling junctions[9,10,11]. There, the particle energy deposited in the crystal produces nonthermal phonons, either indirectly by ionization processes, or directly by the interaction with the lattice nuclei. The latter process is especially of interest because it allows to detect efficiently poorly ionizing recoil events, opening the way to sensitive detectors for dark matter search[12] and coherent neutrino scattering[13].

In this paper, we present coincident measurements of two Sn-junctions evaporated on a (0,0,1) silicon crystal. The FWHM energy resolution of our best Sn-junction was 80 eV for 6 keV X rays absorbed directly in the films. We have seen correlated events between the two Sn-junctions originating from 6 keV X rays absorbed in the silicon substrate. No 6 keV events were seen when illuminating the 280 μm thick silicon substrate from the back. We have investigated the possibility to enhance the phonon sensitive area by connecting two and

three junctions in series to the same preamplifier. It turns out that the excess quasiparticle current has to tunnel through all junctions, making the detector rise time prohibitively long. This result is discouraging for attempts to make large junction arrays[9]: each junction of the array would require its own preamplifier.

In order to study the ionization induced phonon properties, the silicon substrate was illuminated by the more energetic 4 MeV alpha particles. Virtually all events lead to coincident signals in the two junction detectors. The scatter plots obtained when plotting the amplitude of the two detectors against each other show detailed structures. A Monte Carlo calculation, taking into account phonon focussing, was performed to simulate our detector configuration by tracing the ballistic phonons from the point of emission to the location of the two detectors. The calculated scatter plots also show detailed structures indicating that the experimental scatter plots probably do originate from the anisotropic phonon propagation. However, the agreement is qualitative only, the structures are sufficiently different suggesting that the experiment cannot be explained be simple bulk phonon propagation alone. Another disagreement is the much larger measured time difference of the order of several 100 nsec between the two coincident signals, compared to the expected few nsec for bulk ballistic phonons propagating at the speed of sound, around 5000 m/sec in silicon.

However, regardless of the specific nature of those phonons, our measurements do indicate that a substantial fraction of the energy deposited by the ionizing radiation is converted into nonthermal phonons with an energy of at least the required threshold of $2\Delta_{Sn}$. More than 60 % of the deposited energy appears in the form of excess quasiparticles in the superconducting films. Hence, the nonthermal phonon crystal particle detector remains a promissing possibility. However, because the superconducting tunneling junction area is intrinsically limited[14] to small areas, say 100 x 100 μm^2, one has to find a more efficient way of detecting those phonons.

2. Junction fabrication and experimental set-up

The superconducting tunneling junctions were fabricated[15] by thermal evaporation of tin onto either fused silica (13 x 7 x 0.5 mm^3) or the (0,0,1) surface of a single crystal silicon substrate (13 x 7 x 0.28 mm^3, 5 - 15 Ωcm, 10^{15} - $3 \cdot 10^{15}$ impurities/cm^3, optically polished on one side) . Between the two Sn films (film thicknesses: 150 and 250 nm) an insulating barrier was produced by oxidizing the first film under a DC glow discharge[8]. The junction geometry was defined by a photolithographic mask (fig.1) consisting of two photoresist layers separated by a thin (100 Å) film of aluminium. The bottom layer was entirely exposed to UV light. The area to be cut was exposed in the top one as well. A chemical attack then only left photoresist in the area to be protected, creating a photoresist mask. The undercut in the lower layer was extensive, so that during the lift off process the top Sn film cannot tear the oxide barrier

which otherwise would lead to undesirable current leaks in the junction. The two films were evaporated under two different angles, +/- 60^{o} relative to the substrate normal. The resulting displacement of the two films allowed then to contact the two films separately. A scanning electron microscope picture of such a junction is shown in figure 2. The overlapping region of the junction is 50 x 36 μm^2 and the contact leads are 20 µm long and 5 µm wide. The conductivity $\sigma = (R_N \times \text{overlap area})^{-1}$ of the oxide barrier of the junctions varied between $1 \cdot 10^{-4}$ and $3.7 \cdot 10^{-4}$ $\Omega^{-1}cm^{-2}$, where R_N is the normalconducting resistance of the junction. The bias current was typically 250 pA at the operating temperature of 0.37 K and the dynamic resistance R_D of the order of 1 MΩ. This photolithographic lift-off technique, together with the evaporation under different angles, allowed us to fabricate any number of junctions, separated by only a few µm, with sufficiently reproducible high quality current voltage characteristics.

The substrates were mounted into a ^{3}He-cryostat with a base temperature of 0.37 K, where they were exposed either to a ^{55}Fe source, emitting 5.89 keV (Mn K_α) and 6.49 keV (Mn K_β) X rays, or to an ^{241}Am foil, emitting 4 MeV alpha particles. A magnetic field of several 10 Gauss was applied parallel to the oxide barrier in order to suppress the DC component of the Josephson current, which is 5 orders of magnitude larger than the thermal quasiparticle current at the operating point of the detector. The excess quasiparticle current[8,16] induced by the absorption of an ionizing event was integrated by a charge sensitive preamplifier (silicon JFET Sony SK252 followed by an AMPTEK A250). The preamplifier was cooled to 130K to optimize the signal to noise ratio. In the coincidence measurements, each junction was connected to its own preamplifier at 130 K and biased independently. The output was amplified with a pulse shaping time of 2 µsec. With no detector connected to the input, the equivalent noise charge of the system was 400 electrons.

The data acquisition assigned each detector event three values, depending on the measuring mode. When measuring the energy resolution of a single junction those three values were: the signal amplitude, a value proportional to the rise time of the signal and the amplitude of a test pulse delayed by 100 µsec. In the coincidence measurements the following three numbers were recorded: the signal amplitude of the start junction, the signal amplitude of the coincident stop signal (coincidence window: 60 µsec) and a value proportional to the time difference of the two coincident signals. As a cross check, we interchanged start and stop and obtained symmetrical results.

3. Energy Resolution and Connecting Junctions in Series

To investigate the energy resolution of our Sn tunneling junction detectors, we exposed them to the 6 keV X rays of the ^{55}Fe source and used fused silica as a substrate. This way the junctions are sensitive only to X rays absorbed in the Sn films[8]: the energy of an X ray absorbed in fused silica is

immediately thermalized and, hence, at T=0.37 K below the Cooper pair breaking threshold[9]. From the 10 junctions on fused silica, all were sensitive to the X rays with the FWHM energy resolution at 5.9 keV being typically between 100 and 200 eV. The best energy resolution obtained in this series of measurements was 80 eV, shown in figure 3. The contribution of each film could be clearly separated owing to the difference in rise times[8,16], which were of the order of 10 µsec. The collected charge in our best case (fig.3) was $1.8 \cdot 10^6$ electrons, which represents 18% of the theoretically maximal number Q_o of excess quasiparticles produced by 5.9 keV in Sn ($Q_o = E/\Delta_{Sn} = 10^7$ e, where Δ_{Sn}=0.58 meV). The measured effective minimal ionizing energy of our best Sn detector is hence ε = 3.2 meV.

The theoretical Poisson limited FWHM energy resolution at 6 keV of a detector with a minimal ionizing energy of 3.2 meV would be 10 eV. In our measurements, the energy resolution is still limited by electronic noise, owing to the large impedance of the detector. However, there are indications that for the Sn-junction detectors fabricated in the manner described above, the limiting energy resolution[7,8] is 40 eV, most probably due to geometrical inhomogeneities. We did not intend to investigate, and improve, the energy resolution of these devices, but focussed on the possibilities of increasing the size of these detectors. As has been discussed in detail in references[9,14], the area of high quality junctions are limited to the order of 100 x 100 µm^2 because of the influence of the low detector impedance on the system noise. To cover a large area a large number of preamplifiers would be required.

One approach would be to connect several detectors to the same preamplifier. A parallel connection of n junctions is excluded because the total capacity increases to $n \cdot C_D$ and the dynamical resistance reduces to R_D/n, increasing the system noise accordingly (C_D is the capacity and R_D the dynamical resistance of one junction). The signal amplitude will remain constant as long as $n \cdot C_D$ is still much smaller than $A \cdot C_F$, where C_F is the feedback capacity and A the open loop gain of the charge sensitive preamplifier. Connecting the junctions in series will lead to a capacity of C_D/n and a dynamical resistance of $n \cdot R_D$ and the system noise will, in principle, be reduced by a factor of 1/n. However, the signal amplitude will be reduced by the same amount because the n junctions in series act as voltage dividers. Hence, connecting an arbitrary number of junctions in series would yield the same signal to noise as a single junction, if the system noise is determined by the series noise owing to the voltage fluctuations at the input of the FET[14].

We connected two junctions in series, with individuel FWHM energy resolutions at 5.89 keV of 80 eV and 84 eV, respectively. The contributions of the two detectors can be separated clearly because of their different rise times, as is apparent in the rise time versus signal amplitude scatter plot in figure 4. In addition, either film of each junction leads to a different rise time leading to overall 4 individual spectra in figure 4. Connected in series, the K_α peak corre-

sponds to $1 \cdot 10^6$ e, which is approximately the half of the accumulated charge of a single junction. The width of the K_α peak did, however, not decrease, leading to an energy resolution of 180 eV FWHM. This indicates that we were not limited by the series noise in our measurements.

In addition, the rise time was 20 μsec, twice as long as for of a single junction. On another substrate with slightly poorer quality junctions (single junction rise times of the order 15 μsec), we connected three junctions in series and observed typical rise times of the order of 50 μsec. Those increasing rise times with increasing number of junctions connected in series cannot be explained by simple RC considerations alone. In a charge sensitive amplifier the rise time of the output signal is proportional to the decay of the signal current to be integrated (the intrinsic response time of our charge sensitive amplifier is 50 nsec). On the other hand, the decay of the excess quasiparticle current is given by the tunneling time[14] τ_{tun} of the junction, which is the fastest quasiparticle relaxation mechanism at the low operating temperatures where thermal quasiparticle recombination is negligible[16]. It appears that the time it takes to transport the excess quasiparticle current through the chain of n junctions connected in series is roughly proportional to $n \cdot \tau_{tun}$. Because Cooper pairs cannot transport charge across the junction, owing to the magnetic field applied parallel to the oxide layer, quasiparticle tunneling has to account for the transport of the current through the chain of n junctions. For a large number of junctions connected in series this becomes a prohibitively slow process.

4. Coincidence Measurements on Silicon

As has been pointed out in the introduction, superconducting tunneling junctions can be used as phonon sensitive devices on a crystal, in which the deposited energy excites nonthermal phonons with energies of at least 2Δ, the Cooper pair binding energy of the superconducting film. At the low operating temperatures of junction detectors, those nonthermal phonons can propagate large distances because of the long spontaneous phonon decay time at the threshold energy 2Δ of the junction. This decay time has a $(\hbar\omega)^{-5}$ energy dependence[17], consequently high energy phonons ($\hbar\omega_{Debye}$) decay fairly fast to phonons with lower energies, but live sufficiently long at the threshold energy 2Δ. For a Sn-junction on silicon this lifetime at the threshold energy is 3.8 msec[18]. Competing anharmonic phonon relaxation mechanisms are due to impurities and grain boundary scattering and diffuse scattering of the crystal surface[17]. We have therefore proposed[18] to fabricate anisotropically etched structures from a low impurity silicon ($\sim 10^{14}$ impurities cm^{-3}) to reduce those mechanisms.

When two junctions, evaporated on the same substrate and each with its own preamplifier, show simultaneously signals induced by a radioactive source, the information must have been mediated by the phonons of the substrate.

Hence, coincident measurements provide information on the production of phonons in the substrate by radiation, their transport through the crystal and the transmission into the superconducting film. As has already been apparent in reference[8], all these processes must be fairly efficient, because from the Sn-junction ^{55}Fe spectra on silicon one sees that the pulse height of the phonon induced signals are only smaller by a factor of two relative to the pulse heights of events absorbed in the superconducting events directly.

We measured the coincidence signals in a time window of 60 μsec between two superconducting tunneling junctions, the substrate of which was exposed to a ^{55}Fe 6 keV X ray source. The substrate was either illuminated from the front (the surface onto which the junctions were evaporated) or from the back side. In figure 5, the scatterplots of the pulse heights of the coincident junction signal against the pulse height of the triggering junction signal is shown for the two edge-to-edge separations of 5 μm and 30 μm, respectively. The values are given in units of collected charge as calibrated with a test pulse in a capacitor at the input of the charge sensitive preamplifier. The events with large pulse height A_1 and small pulse height A_2 are due to a deliberate low discriminator threshold allowing noise to be correlated with events directly absorbed in the film for calibration purposes. It is evident from figure 5 that the number of truly coincident signals, the triangle in the lower left part of the scatter plot, decreases with increasing junction separation. A histogram of the time separation of the coincident signals from two junctions separated by 5 μm is shown in figure 6. A cut in the pulse height of the coincident signal has been applied to reject the noise correlated data from events absorbed directly in the film. Above a residual background of accidentals, consistent with the individual count rate of 30 Hz, a peak of truly coincident events centered around $\Delta t=0$ and a FWHM of 450 nsec appears. This width is larger than the time resolution of our system which is 250 nsec. No X ray induced signal has been seen in either junction when the substrate (Si 280 μm thick) was exposed to the ^{55}Fe source from the back.

The same experiment has been repeated for ^{241}Am alpha particles illuminating the silicon crystal from the back side. The energy distribution of our alpha source, a foil with ^{241}Am and a gold protection layer, was measured with a silicon surface barrier detector. It showed a broad peak with a maximum at 4 MeV. The particle energy is fully deposited after about 20 μm in silicon. A scatter plot of the pulseheights of the correlated signals of the two detectors is shown in figure 7. The junction separation is 30 μm. Again, the units are in collected charge. Distinct bands are visible in the scatter plot: three major bands, labeled 1-3 in figure 7, each showing additional fine structure. The distribution of the time difference between the two coincident alpha signals is shown in figure 8, where the peaks correspond to the bands in figure 7.

In order to understand the scatter plot of fig.7, we have simulated the phonon propagation in our detector configuration with a Monte Carlo calculation. In a silicon crystal of 280 μm thickness, ballistic phonons are emitted in a depth of z = 270 μm relative to the surface with the junction. This is roughly the energy deposition region of the alpha particles when illuminated from the back side. The (x,y) coordinate of the phonon emission point is selected randomly, reflecting the fact that in the experiment the entire crystal surface is hit by the alpha particles. The direction $\vec{n} = \vec{k}/|\vec{k}|$ of the phonon with wave vector $\vec{k}$ and phase velocity $\vec{v}_k$ is chosen isotropically. The energy of the propagating phonon wavefront, however, is transported in the direction of the phonon group velocity $\vec{v}_g^{\alpha} = \partial\omega^{\alpha}(\vec{k})/\partial\vec{k}$, where $\omega^{\alpha}(\vec{k})$ is the constant-frequency surface of the phonon. The index α corresponds to the polarization ε_{α} of the phonon, where α=0 corresponds to the longitudinal mode (LA), α=1 to the slow transverse (STA) and α=2 to the fast transverse (FTA) mode. In the long wavelength limit ($\lambda \gg$ lattice constant), the medium can be modeled to be continuous but anisotropic. Phonon propagation is then determined by a generalized statement of Hookes law: $\sigma_{ij} = \sum c_{ijkl} e_{kl}$, where σ_{ij} is the stress, e_{lm} the strain and c_{ijkl} the elasticity tensor of the medium. For a crystal with cubic symmetry, as is the case for silicon, just three independent parameters define the nonzero elements: $c_{iiii}=C_{11}$, $c_{iijj}=C_{12}$ and $c_{ijij} = c_{jiji} = C_{44}$. From the appendix of the paper of Northtrop and Wolfe[13] one can deduce the expression for the phonon group velocity $\vec{v}_g^{\alpha}$, which is a complicated combination of the elasticity tensor components c_{ijkl} and the direction $\vec{n}$ of the wave vector.

In the simulation, we took the junction area to be 50 x 50 μm^2 and the separation between the two junctions was 30 μm. The phonons were assumed to propagate without losses in the medium and are absorbed on the surface (i.e. no phonon reflections at the surface). The results are presented as scatter plots in figure 9, for the case of isotropic phonon propagation and for the three phonon polarizations in the case of phonon focussing. In each scatter plot, the number of phonons hitting junction 1 is plotted against the number of phonons hitting junction 2 for each event. A total of 10^6 phonons have been emitted randomly per event. Each scatter plot corresponds to 15000 events which are distributed randomly in a plane of 1.5 x 1.5 mm. In the case of phonon focussing, detailed structures appear in the scatter plots. There is qualitative agreement between the calculated structures for the LA and FTA modes and the measured scatter plots (fig.7). In the calculations, the time differences between the pulses are of the order of a few nsec, which is in disagreement with the 450 nsec observed in the experiment (fig.8). Possibly, the phonon pulse is slowed down by multiple scattering, whereby after each scattering event the phonon is refocussed into its original direction of propagation leading to a possibly quasiballistic nature of the nonthermal phonons.

From the scatterplots one can obtain an estimation for the overall efficiency of converting the deposited particle energy into nonthermal phonons and collecting them as excess quasiparticles in the superconducting film. The energy collected in the superconducting tunneling junction is given by following expression

$$E_{coll} = \eta_{trans} \cdot \eta_{geom} \cdot \eta_{2\Delta} \cdot E_{dep} \qquad (1)$$

where
η_{trans} : phonon transmissivity from crystal into film
η_{geom} : geometrical collection efficiency
$\eta_{2\Delta}$: fraction of energy going into phonons with $\hbar\omega > 2\Delta$
E_{dep} : energy deposited by particle

On symmetry reasons the coincident events with largest equal pulse height correspond to events where the energy is deposited between the two junctions. With the help of the Monte Carlo simulation one can then obtain the geometrical factor η_{geom}. Because the junctions are calibrated with the 6 keV X rays absorbed directly in the films, one can express E_{coll} in units of keV. From (1) one deduces an effective efficiency $\eta_{eff} = \eta_{trans} \cdot \eta_{2\Delta}$. The results are presented in table I. Assuming isotropic phonon emission, the efficiency is 80 % for 6 keV X rays absorbed on the front side (maximal coincident signal for X rays absorbed at a depth of 7.5 μm). When absorbing 4 MeV alpha particles at a depth of 270 μm, an effective efficiency η_{eff} of 64 % has been determined for the isotropic case. The focussing and defocussing effects for anisotropic phonon propagation lead to different values for η_{geom} for the three polarization modes. As a consequence η_{eff} varies between 48 % and 192 %. The unrealistic values larger than 100 % again indicate that phonon propagation cannot be described by pure ballistic behaviour.

5. Conclusion

Superconducting Sn/Sn-ox/Sn junctions were fabricated by thermal evaporation and using a two layer photolithographic and an angular evaporation technique. A best FWHM energy resolution of 80 eV at 6 keV was obtained for X rays absorbed directly in the junction films. Connecting junctions in series to the same FET of the charge sensitive preamplifier lead to an increase in signal rise time roughly proportional to the number of connected junctions. Hence, for achieving a high energy resolution in each pixel of a superconducting tunneling junction array detector, each pixel would require an individual electronic read out.

Junctions with edge-to-edge separations between 5 and 30 μm were fabricated on silicon substrates to detect the common nonthermal phonon wavefront induced by energy deposited in the substrate. When illuminating the detec-

tor from the front, correlated 6 keV X ray events were seen. No X rays were detected in the case of back side illumination. Experiments with 4 MeV alpha particles absorbed in the back side of the substrate show structures in the pulse height scatter plots of the two coincident signals. These results were compared with a Monte Carlo calculation simulating ballistic phonon propagation in an anisotropic medium. The pattern produced by the FTA polarization mode shows some similarity with experiment but the relative time differences between the coincident signals in the calculation are shorter by more than one order of magnitude. With the geometrical phonon collection efficiency taken from the Monte Carlo calculation one obtains a value around 60 % for the energy collection efficiency of this crystal/junction detector.

Our experiments confirm the feasibility of a combined crystal/superconducting film detector in which one looks for excess quasiparticles produced by nonthermal phonons from the substrate. However, the small intrinsic size of the order of 100 x 100 μm^2 of tunneling junctions remains a problem in any practical application, since each junction needs an individual readout. Nevertheless, the high efficiency of the nonthermal phonon detector principle continues to make it an interesting candidate for a future detector with high sensitivity for nonionizing events.

Acknowledgements

We would like to thank Piero Martinoli and his group for supplying us with the photolithographic technology. We are also grateful to Christian Hèche and his team for the design and construction of the ^3He cryostat. The material presented here is part of the doctoral thesis of one of the authors (Y.d.C). This work was supported by the Swiss National Science Foundation.

References

1) D.McCammon, M.Juda, J.Zhang, S.S.Holt, R.L.Kelly, S.H.Moseley and A.E.Szymkowiak, Proceedings LT 18, Kyoto 1987, Japanese Journal of Applied Physics, 26 (1987), Supplement 26-3.
2) E.Fiorini and T.O.Niinikoski, Nucl. Instr. and Methods, 224 (1984) 83.
3) N.Coron, G.Dambier, G.J.Focker, P.G.Hansen, G.Jegoudez, B.Jonson, J.Leblanc, J.P.Moalic, J.L.Ravn, H.H.Stroke and O.Testard, Nature 314 (1985) 75.
4) G.H.Wood and B.L.White, Appl.Phys.Lett. 15 (1969) 237.
5) D.Twerenbold, Europhysics Letters, 1 (1986) 209.
6) H.Kraus, Th.Peterreins, F.Pröbst, F.v.Feilitzsch, R.L.Mössbauer, V.Zacek and E.Umlauf, Europhysics Letters, 1 (1986) 161.
7) W.Rothmund and A.Zehnder, in "Superconductive Particle Detectors", ed. A.Barone, World Scientific, Singapore, 1988.
8) O.Twerenbold and A.Zehnder, J.Appl.Phys., 61 (1987) 1.
9) D.Twerenbold, Nucl. Instr. and Meth. A273 (1988) 575.
10) B.Cabrera, J.Martoff and B.Neuhauser, Nucl. Instr. and Meth. A275 (1989) 97.
11) Th.Peterreins, F.Pröbst, F.von Feilitzsch, R.L.Mössbauer and H.Kraus, Phys.Lett.B, 202 (1988) 161.
12) M.W.Goodman and E.Witten, Phys.Rev.D, 31 (1985) 3059.
13) A.K.Drukier and L.Stodolsky, Phys.Rev.D, 30 (1984) 2295.
14) D.Twerenbold, Nucl. Instr. and Meth. A260 (1987) 430.
15) Y.de Coulon, Doctoral Thesis, University of Neuchâtel, Switzerland, 1989.
16) D.Twerenbold, Phys.Rev. B34 (1986) 7748.
17) Y.B.Levinson, in 'Nonequilibrium Phonons in Nonmetallic Crystals', ed. W.Eisenmenger and A.A.Kaphyanski, North Holland, Amsterdam, 1986.
18) Y.de Coulon, D.Twerenbold, J.-L. Vuilleumier and G.A.Racine, Proc. of the II European Workshop on Low Temperature Devices for the Detection of Low Energy Neutrinos and Dark Matter, ed. L.Gonzalez-Mestres and D.Perret-Gallix, Editions Frontières, Gif-sur-Yvette, 1989.

Figur Captions

Figur 1

Schematic of the combination of photolithography and directional evaporation in fabricating the superconducting tunneling junctions.

Figur 2

Scanning electron microscope picture of a Sn/Sn-ox/Sn junction. One can see the overlap area of 50 x 36 μm^2 and the contacts which are 20 µm long and 5 µm wide.

Figur 3

Spectrum of ^{55}Fe X rays from a junction on fused silica. The low energy tail is due to X rays absorbed outside of the overlap region.

Figur 4

Scatter plot of rise time versus collected charge of 2 junctions connected in series to the same preamplifier (fused silica substrate). Four K_α regions are visible: the contributions of each film of the two junctions.

Figur 5

Pulse height scatter plot of the coincident 6 keV X ray signals in units of collected charge for the two junction separations of 5 µm and 30 µm, respectively. A_1 is the pulse height of the triggering junction and A_2 the coincident signal. The threshold for A_2 is somewhat lower than noise, enabling to record X rays absorbed directly in junction 1 for calibration purposes.

Figur 6

The time difference distribution of the 6 keV X ray coincident signals of figure 5 for a junction separation of 5 µm (A_2 threshold larger than noise).

Figur 7

Pulse height scatter plot of the coincident signals in units of collected charge for 4 MeV alpha particles absorbed on the back side (junction separation 30 μm), showing three major branches.

Figur 8

The time difference distribution of the 4 MeV alpha particle coincident signals of figure 7 for a junction separation of 30 μm (A_2 threshold larger than noise). The peaks correspond to the three branches in figure 7.

Figur 9

Scatter plots of coincident Monte Carlo generated events, simulating the irradiation of a silicon substrate with 4 MeV alpha particles from the back side. The effects of isotropic phonon propagation and the three polarization modes in the case of anisotropic propagation are shown. For each event, 1'000'000 phonons were generated. The scales are in units of absorbed phonons.

Table I

	6 keV : front side E_{coll} = 710 eV		4 MeV : back side E_{coll} = 6.9 keV	
mode	η_{geom}	η_{eff}	η_{geom}	η_{eff}
isotr.	0.15	0.80	0.0027	0.64
LA	0.17	0.71	0.0009	1.92
STA	0.11	1.10	0.0034	0.51
FTA	0.09.	1.34	0.0036	0.48

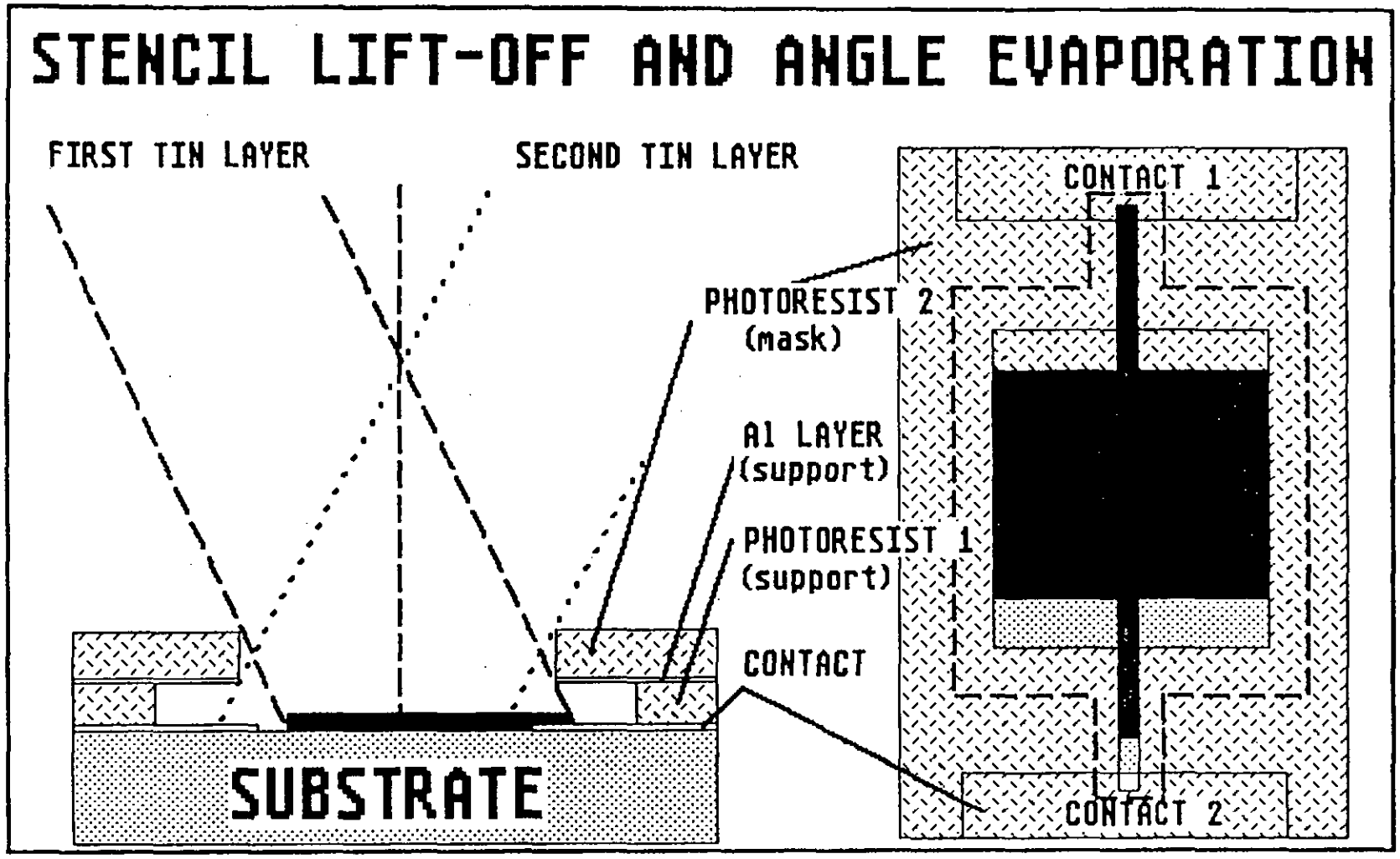
STENCIL LIFT-OFF AND ANGLE EVAPORATION
FIRST TIN LAYER
SECOND TIN LAYER
CONTACT 1
PHOTORESIST 2
(mask)
Al LAYER
(support)
PHOTORESIST 1
(support)
CONTACT
SUBSTRATE
CONTACT 2

figure 1

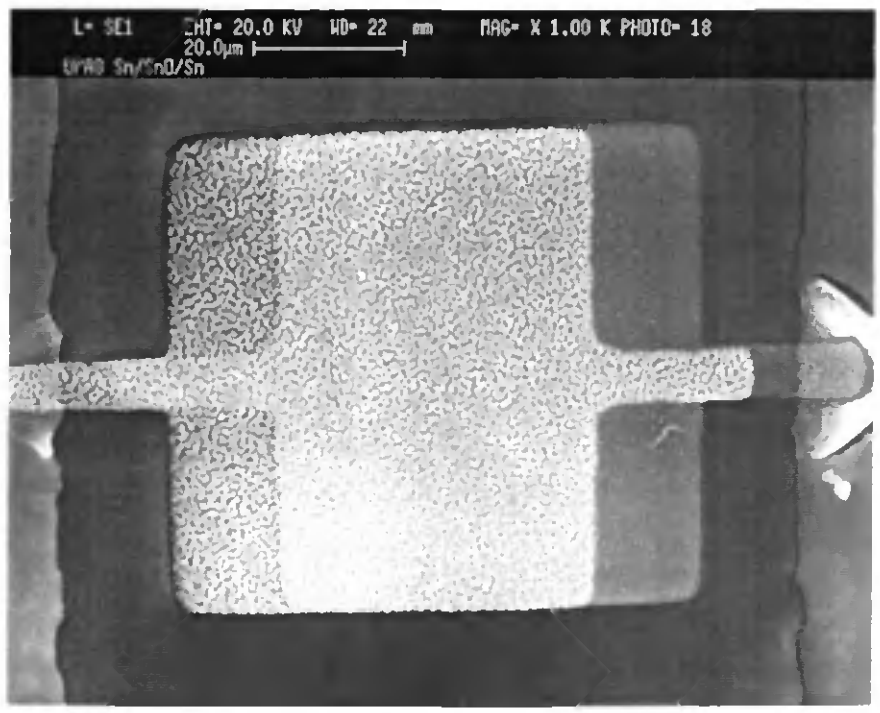

figure 2

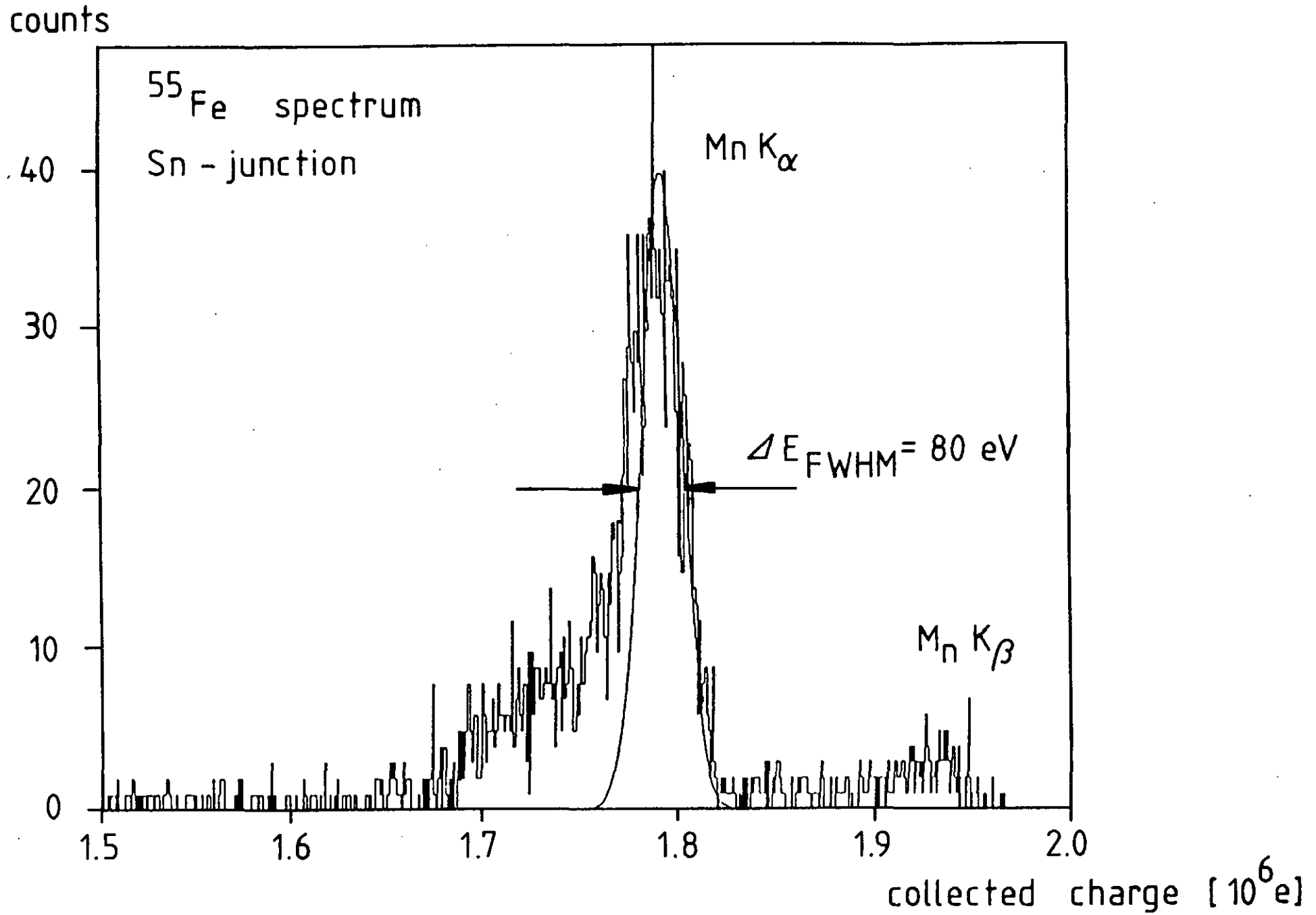
counts
^{55}Fe spectrum
Sn - junction
Mn K_α
ΔE_{FWHM} = 80 eV
Mn K_β
40
30
20
10
0
1.5
1.6
1.7
1.8
1.9
2.0
collected charge [10^6e]

figure 3

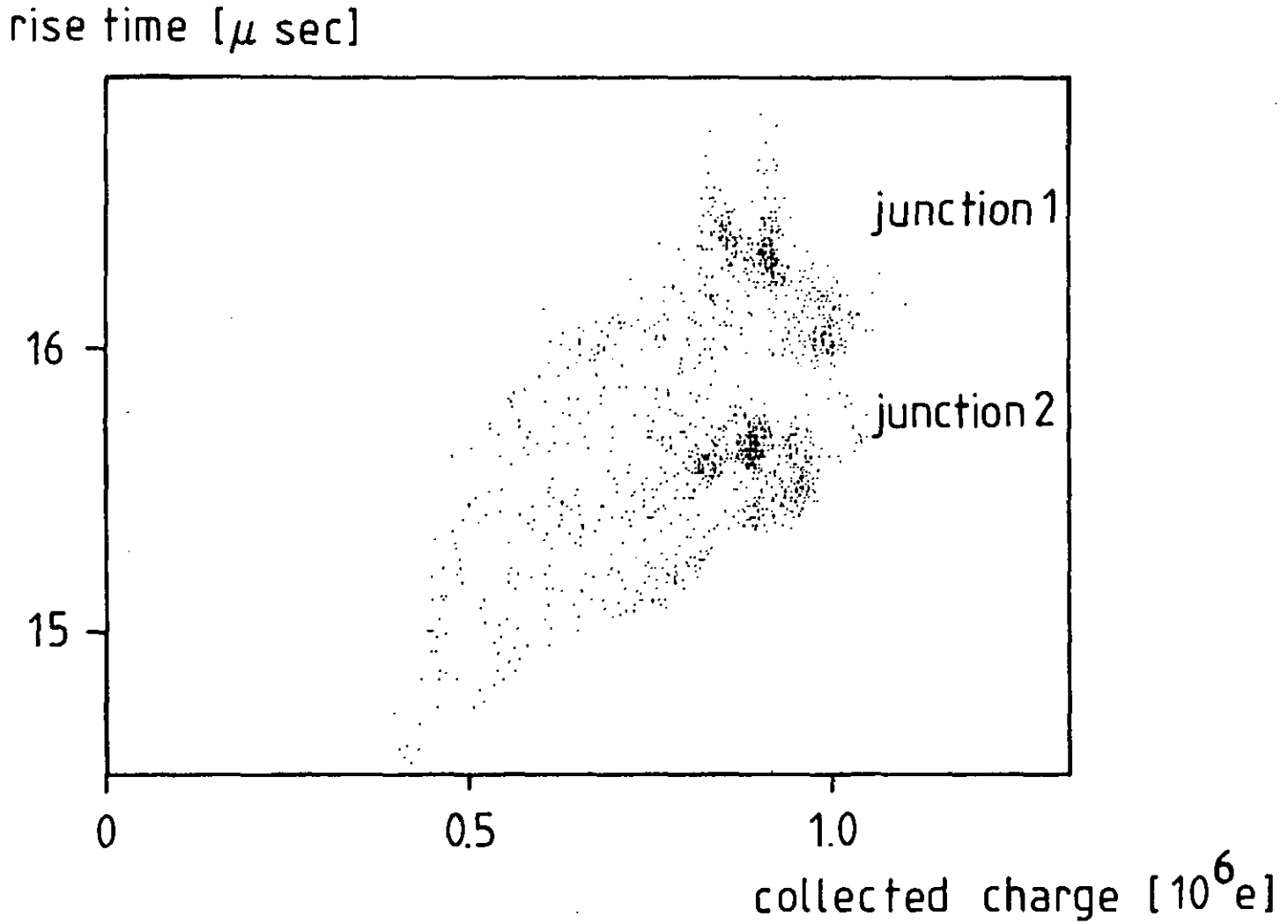
rise time [μ sec]
16
15
junction 1
junction 2
0
0.5
1.0
collected charge [10^6 e]

figure 4

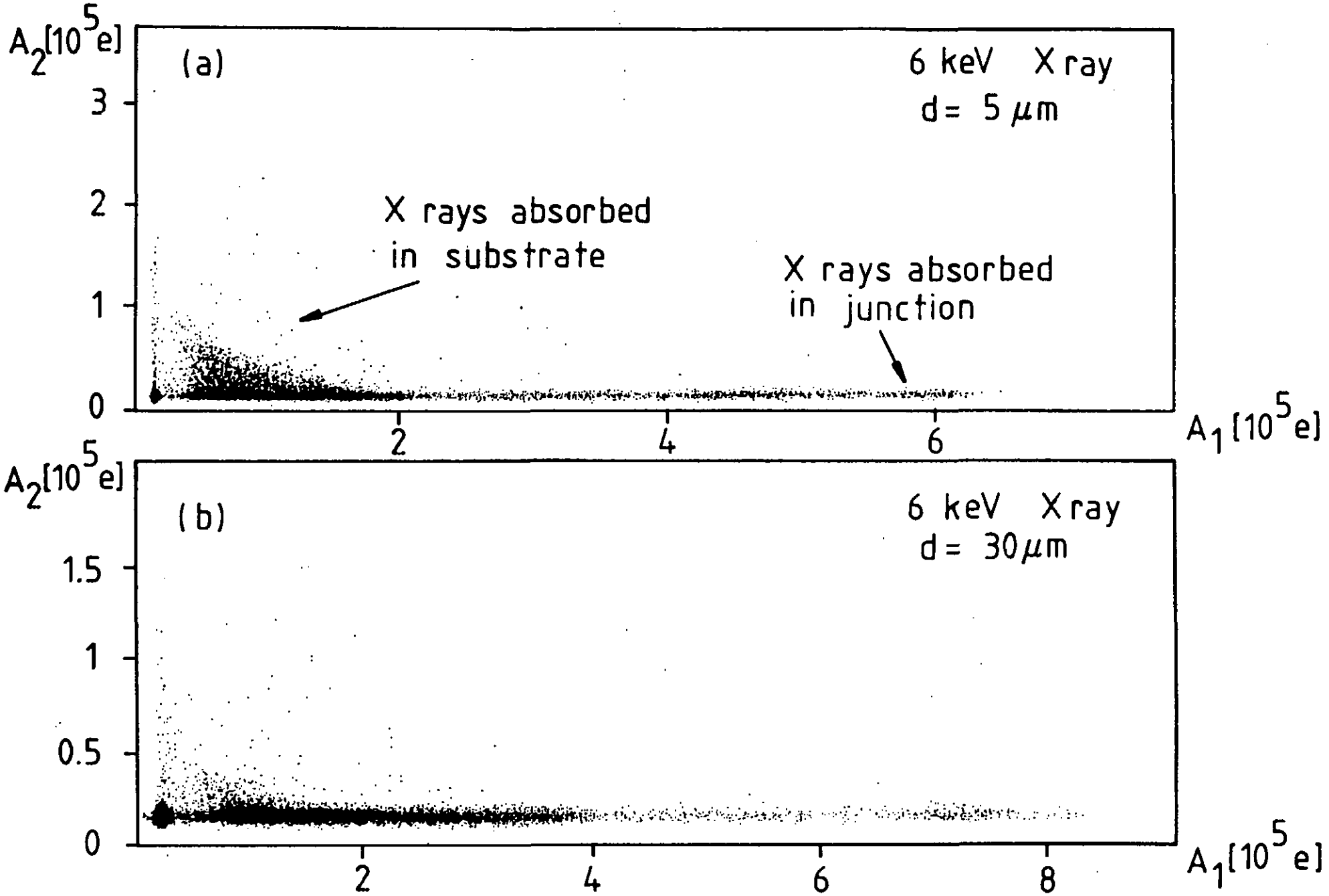
(a)
6 keV X ray
d = 5 μm
X rays absorbed
in substrate
X rays absorbed
in junction
A2[10^5e]
A1[10^5e]
0
1
2
3
2
4
6
(b)
6 keV X ray
d = 30 μm
A2[10^5e]
A1[10^5e]
0
0.5
1
1.5
2
4
6
8

figure 5

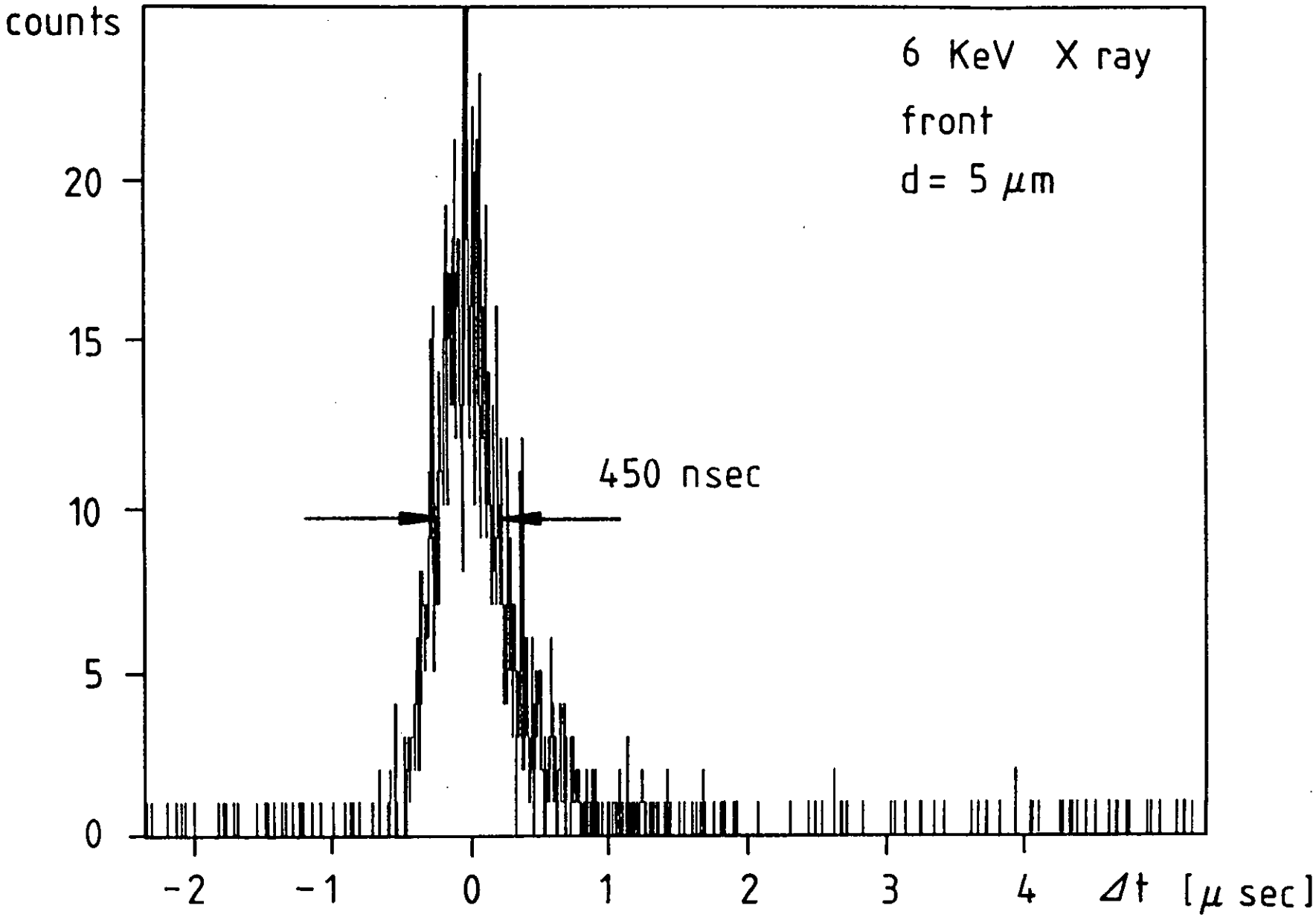
counts
20
15
10
5
0
6 KeV X ray
front
d = 5 μm
450 nsec
-2
-1
0
1
2
3
4
Δt [μ sec]

figure 6

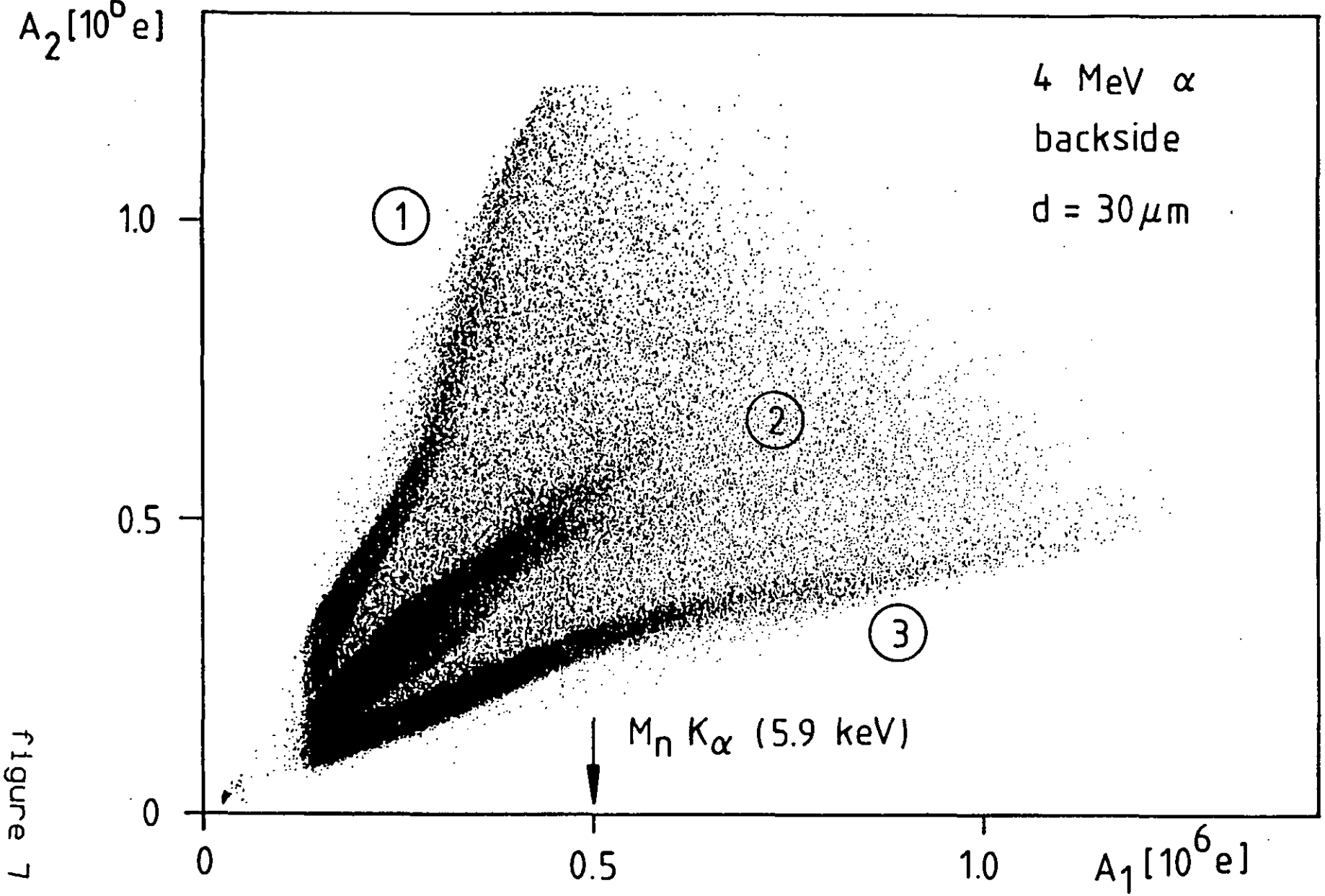
A2 [10^6 e]
1.0
0.5
0
0
0.5
1.0
A1 [10^6 e]
4 MeV α
backside
d = 30 μm
1
2
3
Mn Kα (5.9 keV)

figure 7

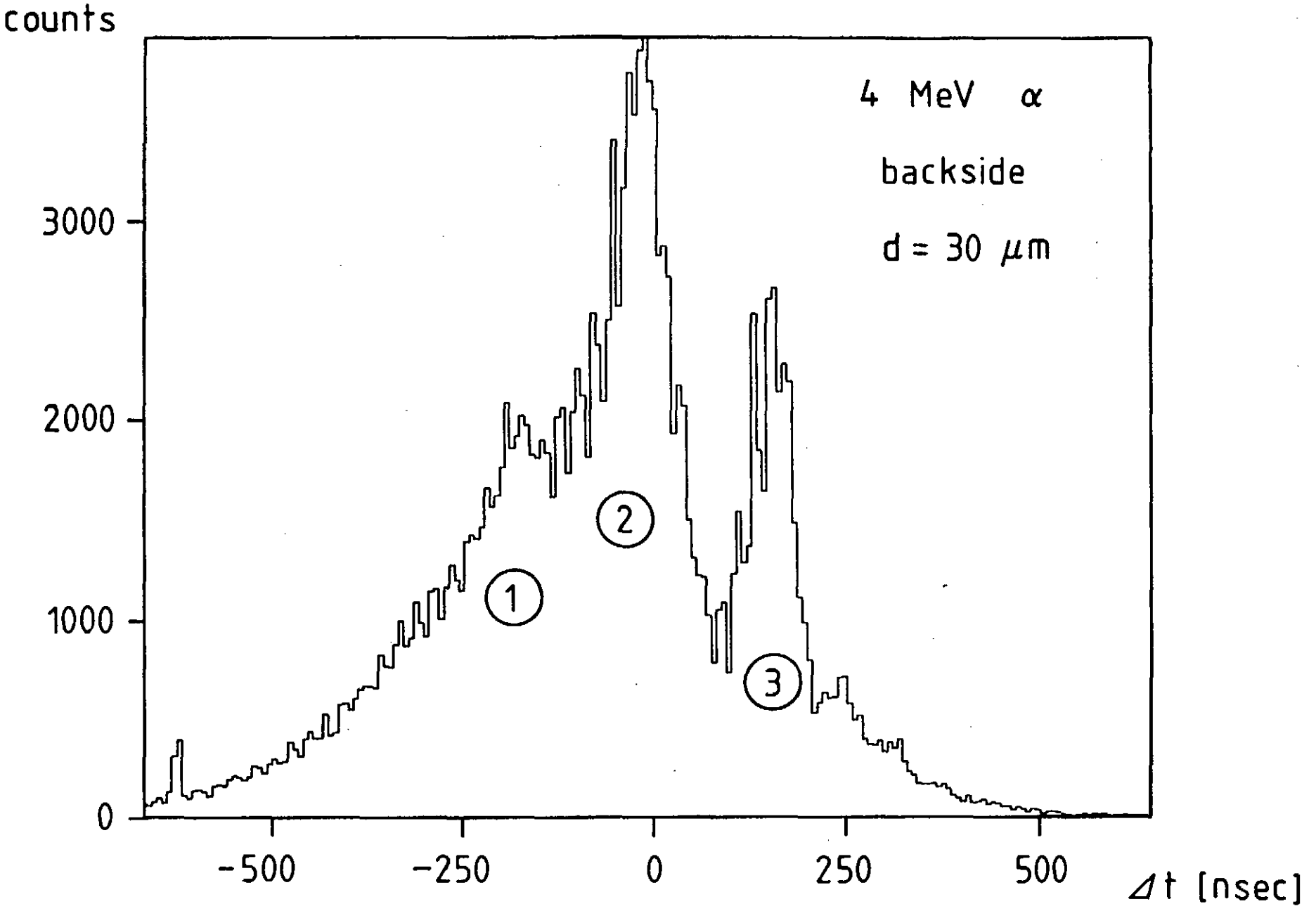
counts
4 MeV α
backside
d = 30 μm
3000
2000
1000
0
-500
-250
0
250
500
Δt [nsec]
1
2
3

figure 8

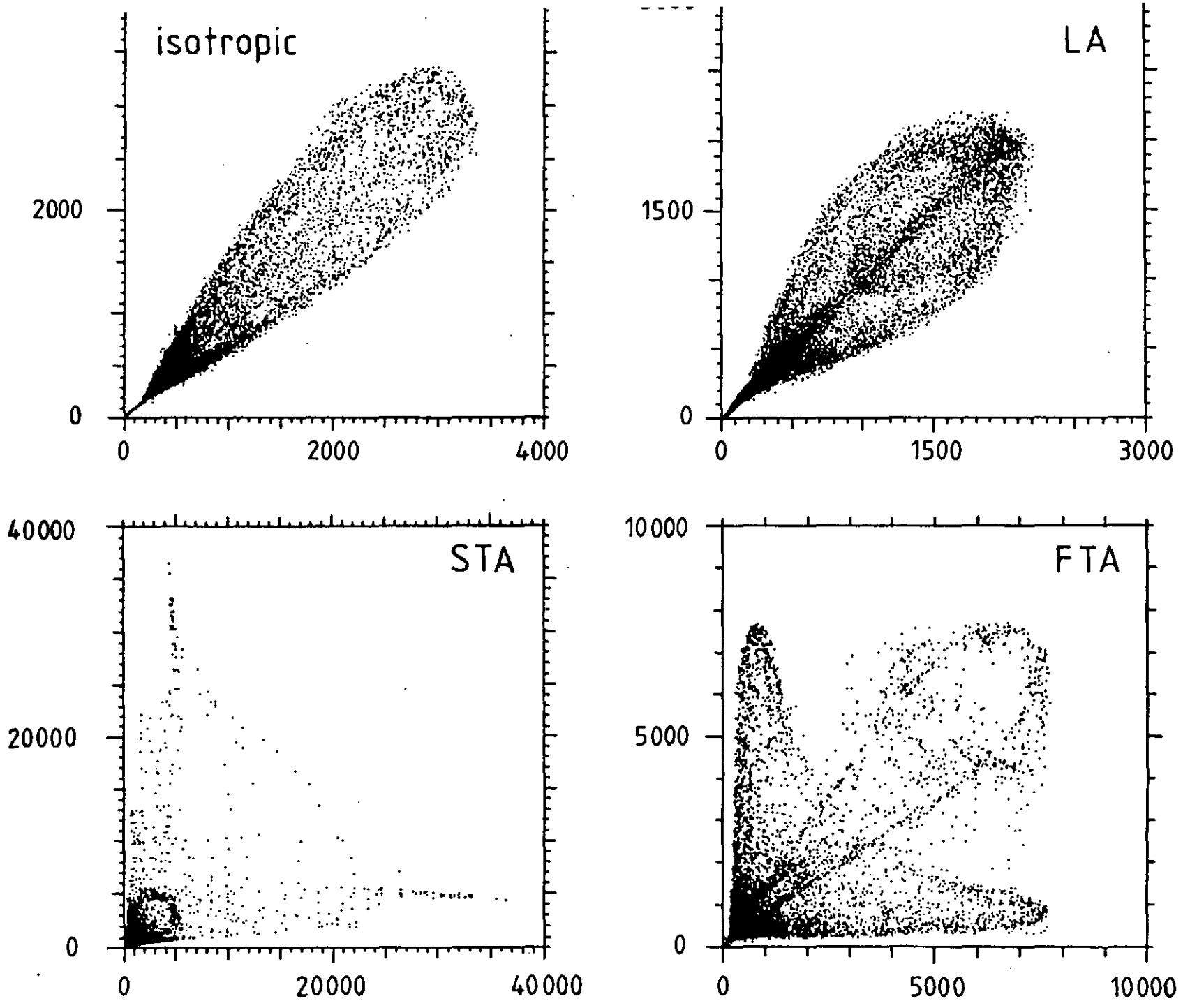
isotropic
2000
0
0
2000
4000
LA
1500
0
0
1500
3000
40000
20000
0
STA
0
20000
40000
10000
5000
0
FTA
0
5000
10000

figure 9